Reducing Bladder Artifacts in Clinical Pelvic SPECT Images

R. Glenn Wells, PhD[1–3]; Troy Farncombe, PhD[4]; Edward Chang, MD[5]; and R. Larry Nicholson, MD[1–3]

[1]Department of Nuclear Medicine, St. Joseph's Health Care, London, Ontario, Canada; [2]Department of Diagnostic Radiology and Nuclear Medicine, University of Western Ontario, London, Ontario, Canada; [3]Lawson Health Research Institute, London, Ontario, Canada; [4]Department of Nuclear Medicine, McMaster University, Hamilton, Ontario, Canada; and [5]Department of Nuclear Medicine, Hôtel Dieu-Grace Hospital, Windsor, Ontario, Canada

SPECT imaging of the pelvis is hampered by the presence of bladder artifacts, which render up to 20% of the images unreadable. The artifacts are caused by the high level of activity in the bladder and by the change in activity level as the bladder fills during data acquisition. The changing activity, together with the inhomogeneous attenuation of the pelvis, leads to inconsistencies in the projections and consequently artifacts when the data are reconstructed with filtered backprojection (FBP). dSPECT is an iterative algorithm that permits the reconstruction of dynamic SPECT images from a single, slow-rotation SPECT data acquisition. The reconstruction algorithm incorporates attenuation correction (AC) and changing tracer distributions and has been shown to reduce bladder artifacts in simulated data. In this study, we showed that dSPECT is effective at removing bladder artifacts from clinically acquired pelvic bone SPECT images. **Methods:** Data from 20 patient volunteers were reconstructed using FBP, rescaled block-iterative reconstruction (RBI) without AC, RBI with AC, and dSPECT. AC was based on patient-specific attenuation maps acquired with a ^{153}Gd scanning line-source transmission system. For dSPECT, 16 time frames (4 projections/head/frame) were reconstructed and then summed to produce the final image. Artifact-to-bone contrast was compared, and image quality was subjectively assessed. **Results:** Compared with FBP, RBI without AC significantly reduced ($P = 0.008$) the streak artifact. Both dSPECT and RBI with AC further significantly reduced ($P < 0.001$) the streak artifact and also improved the uniformity and symmetry of bone tracer-uptake. RBI with AC and dSPECT produced equivalent images if the change in bladder activity during acquisition was modest; however, with large changes in the activity (>100%), RBI with AC did not completely remove the artifact. In that situation, dSPECT produced additional reductions in streak-to-bone contrast. **Conclusion:** Of the methods considered, dSPECT is the most effective at removing bladder artifacts in clinical pelvic SPECT.

Key Words: bladder artifact; bone SPECT; attenuation correction; dynamic SPECT

J Nucl Med 2004; 45:1309–1314

Received Nov. 12, 2003; revision accepted Feb. 5, 2004.

For correspondence or reprints contact: R. Glenn Wells, PhD, Department of Nuclear Medicine, St. Joseph's Hospital, 268 Grosvenor St., London, Ontario, Canada, N6A 4V2.

E-mail: wells@lri.sjhc.london.on.ca

Pelvic imaging using SPECT is plagued by the presence of the "bladder-filling" artifact. Bone imaging of the pelvis is an important diagnostic test for the detection of avascular necrosis of the femoral heads and for the detection of metastatic tumors and other diseases such as osteomyelitis. Planar imaging is possible, but SPECT offers improved sensitivity and specificity because it has greater contrast and allows differentiation of overlying internal structures. When SPECT has been available, its sensitivity in the detection of avascular necrosis has been shown to be 85%, compared with 55% for planar imaging, with no loss of specificity (*1*). Two major obstacles limit SPECT of the pelvis: the inhomogeneous attenuation caused by the hip bones and pelvic girdle and the accumulation of activity in the bladder due to normal excretion of bone radiotracer throughout scanning. Both factors lead to inconsistencies in the projection data, which cause artifacts in the reconstructed image. These artifacts can appear as anomalous blobs of apparent activity, which may be mistaken for tumors (false positives), or as dark shadows, which can hide true lesions (false negatives) (*2*,*3*) and mimic the photon-deficient regions of avascular necrosis (*4*). The bladder-filling artifacts that occur in pelvic imaging are particularly severe, rendering as many as 20% of SPECT scans of this region unusable (*1*).

Attenuation correction (AC) has been shown to improve bone SPECT image quality in other regions of the body, such as the cervical spine (*5*,*6*), and to improve lesion detection in thoracic SPECT (*3*). PET images of the pelvis have also been shown to benefit from AC (*7*). Unfortunately, AC alone may not be sufficient for SPECT because changing activity in the bladder throughout the acquisition contributes to the artifact. Catheterization is a possible means of mediating this effect but has an associated increased risk of complications such as infection and consequently is unattractive for general application. Different techniques of digital filtering have been suggested to correct for this artifact (*4*,*8*) but have had limited success (*9*). These approaches try to correct for the artifact after image creation and do not address the issue of the changing bladder-activity levels. A different approach is that of Penney et al. (*10*), who attempted to reduce the inconsistencies in the data by acquiring multiple fast-rotation images, that is, a dynamic SPECT acquisition. By acquiring 10 complete SPECT scans over the course of 30 min, Penney et al. were able to reduce the artifact by 50%. Faster scans, with even less change in bladder activity from start to finish, should further reduce the impact of the artifact. Unfortunately, fast-rotation continuous imaging, a technique for performing dynamic SPECT, requires specialized hardware and is consequently not available in most nuclear medicine departments.

An alternative method of dynamic SPECT is the dSPECT technique (*11,12*), which uses a standard, slow, single-rotation acquisition and incorporates both attenuation and the evolution of tracer distribution into the reconstruction algorithm itself. Computer simulations of the Zubal phantom have shown that dSPECT can greatly reduce the appearance of bladder-filling artifacts and consequently improve the detectability of pelvic bone lesions (*13*).

In this work, we evaluated dSPECT using clinically acquired pelvic bone SPECT data. Twenty patient datasets were compared using 4 reconstruction methods: filtered backprojection (FBP), rescaled block-iterative reconstruction (RBI) (*14*) (a variant on ordered-subsets expectation maximization) with no attenuation correction (AC), RBI with AC (RBI AC), and dSPECT.

MATERIALS AND METHODS

Twenty volunteers (11 female and 9 male) were recruited from patients already scheduled for bone scanning in our department (University of Western Ontario ethics approval 08105E). Ten patients were symptomatic, having pain or discomfort in the hips, and 10 were asymptomatic in the hips. The average patient age was 59 y. Each patient received 900 MBq of ^{99m}Tc-methylene diphosphonate and was imaged 3–4 h after injection. Our standard imaging procedure was followed, with each patient voiding his or her bladder immediately before imaging.

All data were obtained with a Millennium MG dual-head SPECT camera (General Electric Medical Systems) equipped with a ^{153}Gd scanning line source transmission system. To permit transmission imaging, the heads were positioned in the cardiac configuration, 101° apart. Transmission imaging supplied the attenuation map used in the RBI AC and dSPECT methods. Each dataset consisted of sixty-four 128 × 128 projections per head acquired over 180°, resulting in a total of 281° of projection data. Transmission data were obtained interleaved with the emission data. The total scanning time was 30 min.

Data were reconstructed by 5 methods. The first was FBP, representing the clinical standard for reconstruction. Only a ramp filter was used during FBP so that the same filter could be applied, after reconstruction, to all images. The second was RBI reconstruction, a variation of ordered-subsets expectation maximization reconstruction that has shown some image-quality advantages over it (*15*). Four iterations with 32 subsets were used, approximately equivalent to 128 iterations of the maximum-likelihood expectation maximization (MLEM) algorithm (*16*). To allow comparison of iterative reconstruction alone to FBP, no AC was applied. The third method was the same as the second but with patient-specific AC (RBI AC). The fourth approach was to use dSPECT reconstruction. The dSPECT algorithm has been described in detail elsewhere (*11,12*). It uses the fact that SPECT projections are not all acquired simultaneously but instead are acquired sequentially, with each 2-dimensional projection being taken from a different angle and at a later time. The reconstruction allows the activity in each voxel to independently change over time, with the constraint that its time–activity curve contain at most 1 peak. In our implementation, we used an iterative expectation-maximization algorithm similar to MLEM and constrained the activity to be never decreasing. The data were divided into 16 time frames, each corresponding to 2 min of data, and the equivalent of 48 MLEM iterations was used. The result of the dSPECT reconstruction was a set of sixteen 128^3 images showing the dynamic course of the tracer distribution. However, in this study, the dynamic set of images was averaged to generate a single image that could be compared with those produced by the other reconstruction methods. A lower number of iterations, compared with the RBI algorithm, was chosen to keep total reconstruction time down to 1 h. To confirm that any differences seen between the RBI AC and dSPECT methods was not due simply to a difference in the number of MLEM-equivalent iterations (128 vs. 48), a final method was considered. This last method was RBI AC but with 3 iterations and 16 subsets to give the equivalent of approximately 48 MLEM iterations (RBI AC_low).

In all cases, images were reconstructed into a 128^3 array and then filtered with a 3-dimensional gaussian filter of 2.5 pixels (11 mm) in full width at half maximum. This filter was chosen to provide a final reconstructed resolution similar to that used clinically in our department. Scatter correction was not applied during any of the reconstructions. All images were reconstructed off-line on a Pentium III (Intel Corp.), 1.0-GHz Linux-based personal computer.

All reconstructions were returned to the clinical environment, where they were evaluated subjectively by 2 nuclear medicine physicians, both of whom were familiar with these types of images. They were free to adjust windowing levels and choice of color scale as desired. The images were assessed on a 5-point scale for the presence of artifacts and the clinical impact of artifacts on diagnosis of pelvic abnormalities. Clinical impact related to the location of the artifact; for example, were artifacts present but in a part of the image such that they would not have influenced clinical evaluation of the image (e.g., evaluation for the presence of avascular necrosis)? Clinical impact also referred to the impact of the artifact on overall image quality; for example, was there an increase in image noise distal to the artifact itself? On the 5-point scale, 1 corresponded to low image quality (large artifact and clinical impact) and 5 to high image quality (no visible artifact or clinical impact). Significance was assessed using ANOVA followed by the Scheffé multiple-comparisons test.

The magnitude of the artifact was assessed quantitatively using region-of-interest (ROI) analysis. A square ROI (ROI_{streak}), 5 × 5 pixels, was positioned in the region of the streak artifact, just outside the bladder (Fig. 1). A second ROI (ROI_{bone}) of the same size was positioned over a region of homogeneous, artifact-free bone. Both ROIs were placed on a transaxial slice containing the center of the bladder. Using the 2 ROIs, the contrast of the streak to the bone was calculated as follows:

$$\text{Contrast} = \frac{ROI_{streak} - ROI_{bone}}{ROI_{bone}}. \qquad \text{Eq. 1}$$

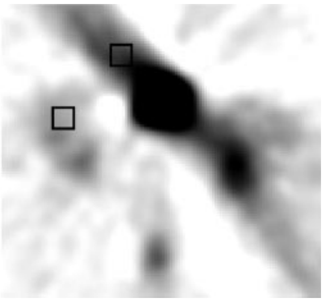

FIGURE 1. Transaxial slices of an FBP-reconstructed image showing typical positions for the ROIs used to contrast the streak artifact (upper ROI) with the bone (lower ROI).

In the absence of a streak artifact, ROI_{streak} should contain only counts from soft-tissue background, and the contrast would approach a value of −1.

For each of the 20 patients in the study, the change in bladder activity was calculated on the basis of the dSPECT-reconstructed dynamic series of images. A bladder volume of interest (VOI) was defined on the summed image using a threshold at 25% of the maximum counts in the bladder. Because activity in the bladder is continually increasing, the change in activity ($\Delta_{bladder}$) is the difference between the counts in the bladder VOI in the last frame and those in the first frame, expressed as a percentage of the VOI counts in the first frame:

$$\Delta_{bladder} = \frac{VOI_{last} - VOI_{first}}{VOI_{first}} \times 100\%. \qquad \text{Eq. 2}$$

RESULTS

Example transaxial slices from 3 patients are shown. The images reconstructed with RBI AC_low did not show any visible differences from those reconstructed with RBI AC and so have not been presented here. The first patient (Fig. 2) was a 47-y-old man presenting with pain in the right knee and elbow but no symptoms in the pelvis. The change in activity in the bladder was 173%, the second largest in the study. This patient's images demonstrated a visible reduction in the streak artifact with the different reconstruction methods. RBI with no AC reduced the magnitude of the streak artifact extending diagonally from the upper left (northwest) to the lower right (southeast) of the FBP image. However, the artifact was still present, both to the northwest of the bladder and to the southeast, as shown by the apparently anomalous and asymmetric uptake in the left acetabulum. RBI AC further reduced but did not completely remove this artifact. In the dSPECT images, the streak artifact was virtually eliminated. Consequently, the contrast between the bladder and the pelvic bones and the left-to-right symmetry also improved.

The second patient (Fig. 3) was a 38-y-old woman presenting with left hip pain. In this patient, the change in bladder activity was 77%. The bladder artifact interfered with the region of interest—the left hip and pelvis—greatly reducing the confidence with which one could assess the diagnosis. Iterative reconstruction alone was insufficient to remove this artifact; AC or dSPECT was necessary. Evaluation of the clinical bone series for this patient provided the following information. Dynamic images taken during tracer injection were normal for this patient, though posterior planar images acquired 3 min after injection showed a subtly increased uptake in the hip. Delayed whole-body images also showed an increased uptake in the inferior acetabulum or ischium. This patient underwent MRI, which found centered on the left ischial tuberosity a mildly expansive heterogeneous osseous lesion whose appearance was most compatible with hemangioma. All these findings supported the validity of the increased uptake seen in the left acetabulum on the RBI AC and dSPECT images.

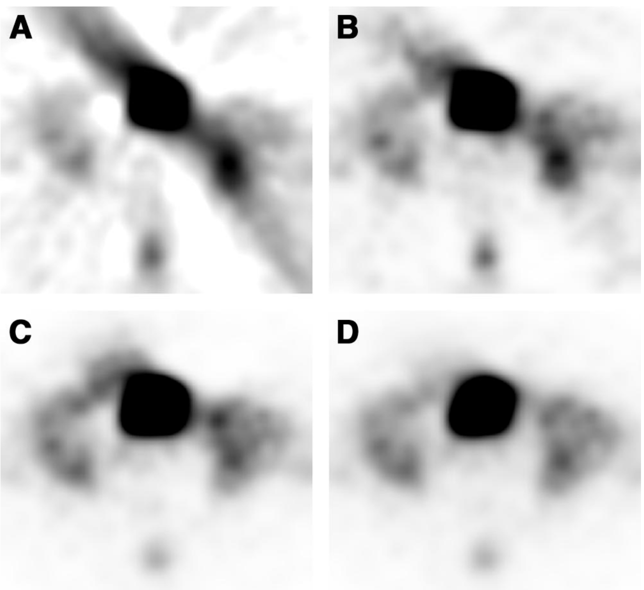

FIGURE 2. Transaxial slices showing an asymptomatic patient with a 173% change in bladder activity. Reconstruction is with FBP (A), RBI no AC (B), RBI AC (C), and dSPECT (D).

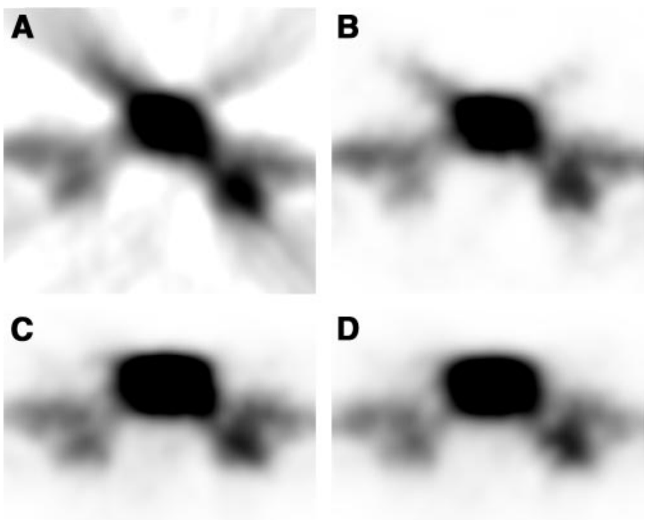

FIGURE 3. Transaxial slices showing a patient with left hip pain and a 77% change in bladder activity. Reconstruction is with FBP (A), RBI no AC (B), RBI AC (C), and dSPECT (D).

The third patient was an 86-y-old woman presenting with central chest pain radiating to her back (Fig. 4). She also described having a lump on the occipital region of her skull. She had a history of breast cancer resulting in mastectomy and, later, cancer in the right hand and thumb. The increase in bladder activity was 88%. A focal lesion on the right side of the pelvis, near the bladder, was visible though subtle with iterative reconstruction but became clear with RBI AC and dSPECT. This focus was not seen on the FBP images. The region of focal uptake was also visible on the anterior whole-body images (shown in Fig. 5 with a 33% threshold) and was consistent with the finding of metastatic disease elsewhere in the skeleton. The SPECT study used a dual-head gamma camera, and consequently, 2 streak artifacts were visible, though one is more intense than the other. The intensity of the streaks depends on the direction of rotation of the camera. Had the lesion been on the opposite side of the body or had the camera rotated in the opposite direction, the influence of the artifact would likely have been even greater.

Shown in Table 1 is the physician evaluation of image quality, averaged over the 20 patients. ANOVA results were similar for both indexes and indicated a significant difference ($P < 0.001$) for each. Subsequent Scheffé multiple-comparisons tests showed, for both indexes, that RBI with no AC performed significantly better than did FBP ($P < 0.001$) and that RBI AC performed significantly better than did RBI without AC ($P < 0.001$). No significant differences were found between RBI AC, RBI AC_low, and dSPECT, though this may have been due to the small number of patients in this study.

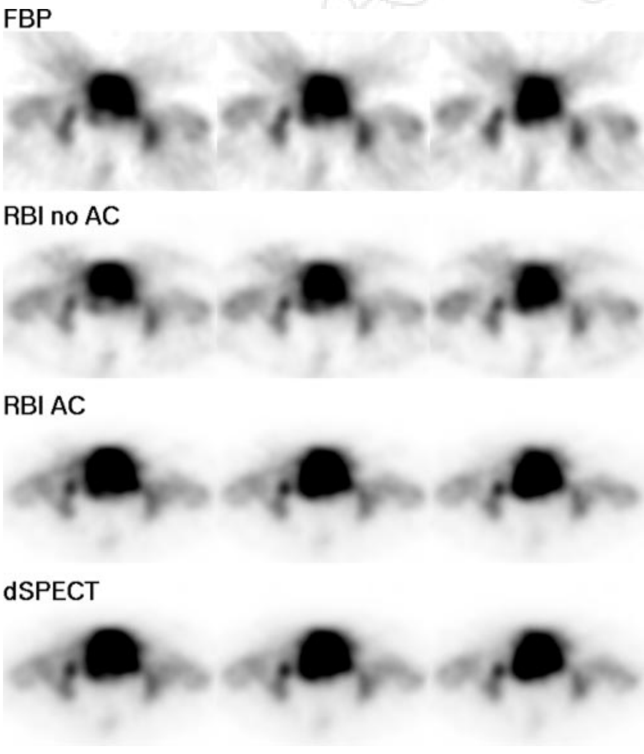

FIGURE 4. Transaxial slices showing a patient with metastatic bone disease and an 88% change in bladder activity. Each row corresponds to 3 consecutive slices of a different reconstruction.

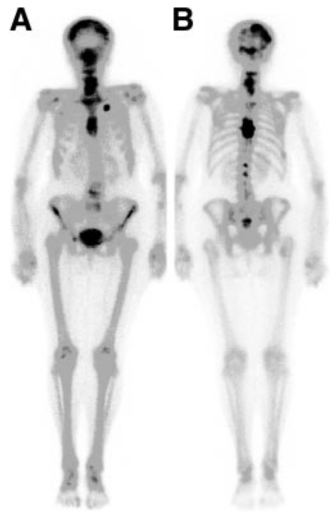

FIGURE 5. Whole-body bone scan of the patient shown in Figure 4 indicating a bone lesion near the bladder. Anterior (A) and posterior (B) views are shown.

The streak-to-bone contrast is shown in Figure 6, with the patients ranked according to the observed change in bladder activity. Ideally, the soft-tissue background activity would be negligible next to the concentration in the bones, leading to a contrast value of -1. The rankings of the contrast as determined with the 5 reconstruction methods were compared using ANOVA and found to be significantly different ($P < 0.001$). A subsequent Scheffé multiple-comparisons test showed that FBP was ranked significantly lower than RBI with no AC ($P = 0.008$), which in turn ranked significantly lower than RBI with AC ($P < 0.001$). RBI AC_low and RBI AC were not significantly different but were significantly lower than dSPECT ($P = 0.03$).

The streak-to-bone contrast measurements mimicked the results of the subjective image quality assessment in that there was an improvement in going from FBP to RBI to RBI AC but little benefit in most patients from using dSPECT rather than RBI AC. However, we did see that for the subset of patients with large increases in bladder activity (>100%) (Eq. 2), and accordingly the worst artifacts, a consistent measurable additional gain was to be had by taking into account the dynamic nature of the bladder activity. In this small study, this subset corresponded to 25% of our patients. With respect to streak-to-bone contrast, that is, artifact removal, dSPECT ranked significantly better than the other methods.

DISCUSSION

RBI AC and dSPECT show a clear advantage in the quality of the reconstructed image, but there is understandably a concern over the price paid in both acquisition time and reconstruction time for these more complicated procedures. These reconstructions use a patient-specific attenuation map, and acquiring the transmission data in an inter-

TABLE 1
Image Quality Evaluation on a Scale of 1 (Poor Image Quality) to 5 (Good Image Quality)

Physician		FBP	RBI no AC	RBI AC	RBI AC_Low	dSPECT
1	Artifact	1.6	3.1	4.2	4.2	4.2
	Clinical impact	1.6	3.1	4.2	4.2	4.2
2	Artifact	1.2	2.7	4.1	4.6	4.5
	Clinical impact	1.6	2.5	4.1	4.3	4.3
Average	Artifact	1.4	2.9	4.1	4.4	4.3
	Clinical impact	1.6	2.8	4.2	4.3	4.2

leaved fashion as we have done increases the acquisition time by 25%. Our final acquisition time of 30 min is still clinically acceptable; however, this additional time could also be avoided through simultaneous transmission imaging or a much faster CT-based transmission system. More important is the increase in reconstruction time. The 128^3 image reconstruction with RBI required 16 min on a Pentium III 1-GHz processor running a Linux operating system. The 4 iterations of RBI with AC (128 MLEM iterations) required 21 min on the same system. Both of these times are acceptable, as they are shorter than the acquisition time of the scan, meaning that they would introduce no additional delays into the daily workflow. The dSPECT reconstruction required 61 min. However, it would not be necessary to reconstruct the entire 128^3 volume dynamically. The bladder occupies approximately only 20–30 slices, and reconstructing just this volume would require correspondingly less time, only 10–15 min. Additionally, personal computers are steadily increasing in performance, and similar machines are now available that run 3–4 times faster than the one used in this experiment.

Scatter correction such as the triple-energy-window (*17*) method might further improve image quality with all of the reconstruction techniques: FBP, RBI, and dSPECT (*18*). It was not possible to apply this type of correction because of

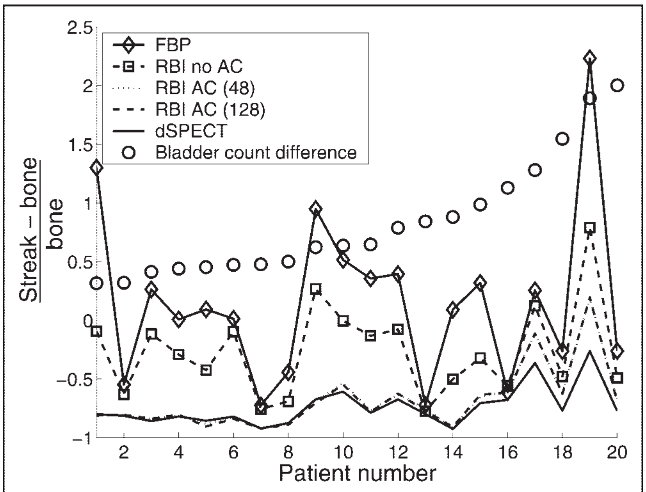

FIGURE 6. Streak-to-bone contrast ranked according to the change in activity in the bladder seen during the data acquisition.

limitations in the data that could be collected with our camera. The transmission system was designed for cardiac acquisitions (64 × 64 projections over a 101° rotation), and it was necessary to restrict the acquisition to 2 energy windows, the photopeaks for ^{99m}Tc and ^{153}Gd, in order to increase the acquisition parameters to 128 × 128 projections over a 180° rotation. Scatter correction via a modeling approach would still be possible, however, with both the RBI and the dSPECT algorithms. Although not expected to alter the main conclusions of this paper, studying the impact of scatter correction on this particular artifact is one direction of possible future investigation.

The use of only 281° of data rather than a complete 360° may have influenced the quality of our reconstructed images. For example, FBP reconstructions from 180° of projection data are well known to have greater geometric distortion in the presence of an attenuating medium than do those from 360° of data (*19*). It has also been reported that angular undersampling can exacerbate bladder-filling artifacts (*20*). These effects are caused by the dependence of the FBP algorithm on the cancellation of counts by negative side-lobes to provide an accurate reconstruction. Because iterative techniques do not rely on this cancellation, they may have been less affected by not having a complete 360° projection dataset, possibly accounting for a small portion of the improvement seen between the results of FBP and those of RBI without AC. The conclusions of this study, however, would remain unchanged with a full 360° of data. Bladder artifacts in pelvic SPECT are known to be caused by the nonuniform attenuating media and changing bladder activity (*20*), both of which also lead to incomplete cancellation of side lobes in FBP, and so iterative reconstruction would be expected to reduce the magnitude of the artifact as was seen in our simulation studies (*13*). Furthermore, as shown in this study, iterative reconstruction alone is insufficient; AC and in some cases dynamic reconstruction are necessary to remove the artifacts.

In addition to its effects in the hip region, radioactivity in the bladder causes artifacts that make assessment of the symphysis pubis and pubic rami difficult in such disorders as osteitis pubis, fractures, and osteomyelitis. Delayed 24-h imaging or catheterization is often required to properly view these bony structures. Although these methods work, they are undesirable from the standpoint of patient compliance and the small but real risk of complications such as infection and trauma. The symphysis pubis and pubic rami of the same 20 patients in this study were reassessed qualitatively by one nuclear medicine physician to determine whether the RBI or dSPECT reconstruction would be beneficial in this region of the pelvis. In 17 of the 20 patients, the symphysis pubis and medial portions of both pubic rami was not interpretable because of either nonvisualization of these pelvic bones (radioactive urine seen instead) or increased uptake, which was considered false positive. In 3 of the patients, streak artifacts were greatly reduced by RBI with AC and dSPECT. Although some benefit was seen through using RBI with AC or dSPECT reconstruction, further improvements in image quality such as with scatter correction or resolution recovery will be necessary before reliable clinical evaluation of the symphysis pubis and pubic rami is possible.

CONCLUSION

In this clinical study investigating SPECT bone imaging of the pelvis, RBI iterative reconstruction with AC and dSPECT were found to perform significantly better than either FBP or RBI with no AC. The bladder-filling artifact was significantly reduced in most patients. In 25% of patients, those with large changes (>100%) in bladder activity, dSPECT was found to provide a measurable additional improvement over RBI AC. Subjective evaluation of image quality did not demonstrate a significant difference between dSPECT and RBI AC, but quantitative analysis of the artifact-to-bone contrast in the hips showed dSPECT to provide a significant advantage.

ACKNOWLEDGMENTS

The authors gratefully acknowledge the assistance of the nuclear medicine technologists and staff at St. Joseph's Health Care (SJHC). This research was supported in part by a grant from the SJHC Foundation, by the Ontario Research and Development Challenge Fund, and by General Electric Medical Systems.

REFERENCES

1. Collier B, Carrera G, Johnson R, et al. Detection of femoral head avascular necrosis in adults by SPECT. *J Nucl Med.* 1985;26:979–987.
2. King MA, Tsui BMW, Pan TS, Glick SJ, Soares EJ. Attenuation compensation for cardiac single-photon emission computed tomographic imaging: Part 2. Attenuation compensation algorithms. *J Nucl Cardiol.* 1996;3:55–63.
3. Wells RG, King MA, Simkin PH, et al. Comparing FBP and OSEM for small lesion detection and localization in Ga-67 SPECT. *J Nucl Med.* 2000;41:1391–1399.
4. Gillen G, McKillop J, Hilditch T, Davidson J, Elliot A. Digital filtering of the bladder in SPECT bone studies of the pelvis. *J Nucl Med.* 1988;29:1587–1595.
5. Case J, Licho R, King M, Weaver J. Bone SPECT of the spine: a comparison of attenuation correction techniques. *J Nucl Med.* 1999;40:604–613.
6. Licho R, Wells RG, King MA. Evaluation of non-uniform attenuation- and scatter-correction in bone SPECT of the cervical, thoracic, and lumbar spine [abstract]. *J Nucl Med.* 2000;41(suppl):328P.
7. Turkington T, Coleman R. Effects of reconstruction methods and attenuation correction on hot bladder artifacts in PET [abstract]. *J Nucl Med.* 2000;41(suppl):194P.
8. Bunker S, Handmaker H, Torre D, Schmidt W. Pixel overflow artifacts in SPECT evaluation of the skeleton. *Radiology.* 1990;174:229–232.
9. O'Connor M, Kelly B. Evaluation of techniques for the elimination of "hot" bladder artifacts in SPECT of the pelvis. *J Nucl Med.* 1990;31:1872–1875.
10. Penney B, Al-Hallaq H, Keast R, Ryan J. Summing rapid SPECT acquisitions reduces bladder filling artifact [abstract]. *J Nucl Med.* 1996;37(suppl):212P.
11. Farncombe T, Celler A, Noll D, Maeght J, Harrop R. Dynamic SPECT imaging using a single camera rotation (dSPECT). *IEEE Trans Nucl Sci.* 1999;46:1055–1061.
12. Celler A, Farncombe T, Bever C, et al. Performance of the dynamic single photon emission computed tomography (dSPECT) method for decreasing or increasing activity changes. *Phys Med Biol.* 2000;45:3525–3543.
13. Farncombe TH, King MA, Wells RG. Reduction of hot bladder artifact in pelvic imaging using single camera rotation dynamic SPECT (DSPECT) [abstract]. *J Nucl Med.* 2001;42(suppl):139P.
14. Byrne CL. Block-iterative methods for image reconstruction from projections. *IEEE Trans Imaging Processing.* 1996;5:792–794.
15. Gifford HC, King MA, Narayanan MV, Pretorius PH, Smyczynski MS, Wells RG. Effect of block-iterative acceleration on Ga-67 tumor detection in thoracic SPECT. *IEEE Trans Nucl Sci.* 2002;49:50–55.
16. Shepp LA, Vardi Y. Maximum likelihood reconstruction for emission tomography. *IEEE Trans Med Imaging.* 1982;MI-1:113–122.
17. Ogawa K, Harata Y, Ichihara I, Kubo A, Hashimoto S. A practical method for position-dependent Compton-scattered correction in single photon emission CT. *IEEE Trans Med Imaging.* 1991;10:408–412.
18. Gur YS, Farncombe TH, Pretorius PH, et al. Comparison of scatter compensation strategies for myocardial perfusion imaging using Tc-99m labeled sestamibi. *IEEE Trans Nucl Sci.* 2002;49:2309–2314.
19. Knešaurek K, King MA, Glick SJ, Penny BC. Investigation of causes of geometric distortion in 180° and 360° angular sampling in SPECT. *J Nucl Med.* 1989;30:1666–1675.
20. Gillen G, Gilmore B, Elliot A. An investigation of the magnitude and causes of count loss artifacts in SPECT imaging. *J Nucl Med.* 1991;32:1771–1776.